JACS
JOURNAL OF THE AMERICAN CHEMICAL SOCIETY
Communication
pubs.acs.org/JACS

Photo- and Thermal-Induced Multistructural Transformation of 2-Phenylazolyl Chelate Boron Compounds

Ying-Li Rao, Hazem Amarne, Leanne D. Chen, Matthew L. Brown, Nicholas J. Mosey, and Suning Wang*

Department of Chemistry, Queen's University, Kingston, Ontario, Canada K7L 3N6

Supporting Information

ABSTRACT: The new N,C-chelate boron compounds B(2-phenylazolyl)Mes_2 [Mes = mesityl; azolyl = benzothiazolyl (**1a**), 4-methylthiazolyl (**2a**), benzoxazolyl (**3a**), benzimidazolyl (**4a**)] undergo an unprecedented multistructural transformation upon light irradiation or heating, sequentially producing isomers **b**, **c**, **d**, and **e**. The dark isomers **b** generated by photoisomerization of **a** undergo a rare thermal intramolecular H-atom transfer (HAT), reducing the azole ring and generating new isomers **c**, which are further transformed into isomers **d**. Remarkably, isomers **d** can be converted to their diastereomers **e** quantitatively by heating, and **e** can be converted back to **d** by irradiation at 300 nm. The structures of isomers **1d** and **1e** were established by X-ray diffraction. The unusual HAT reactivity can be attributed to the geometry of the highly energetic isomers **b** and the relatively low aromaticity of the azole rings. The boryl unit plays a key role in the reversible interconversion of **d** and **e**, as shown by mechanistic pathways established through DFT and TD-DFT calculations.

Molecular isomerism is a common phenomenon in the chemical world. It plays an important role in biology, medicine, and the development of advanced materials.[1−4] The most commonly observed molecular isomerism involves a structural change between two different forms of a molecule, such as the cis/trans isomerization,[2] the interconversion of mer and fac isomers of octahedral complexes,[3] and the transformation between the ring-opened and ring-closed isomers of dithienylethenes and spiropyrans.[4] Because molecular isomerization can often be controlled by external stimuli such as light, heat, or pressure and the different isomers usually have distinct chemical and physical properties, this phenomenon has been exploited extensively in switching/controlling the chemical reactivity and optical, electronic, and physical properties of molecules and materials.[1−4] Although molecular isomerism is common, molecular systems displaying multistructural transformations involving more than two isomers in response to heat or light remain rare. Here we disclose an unprecedented multistructural transformation of organoboron molecules.

This discovery was made during our investigation of a new class of N,C-chelate organoboron compounds, B(2-phenylazolyl)Mes_2 [Mes = mesityl; azolyl = benzothiazolyl (**1a**), 4-methylthiazolyl (**2a**), benzoxazolyl (**3a**), benzimidazolyl (**4a**)] (Scheme 1), which are analogues of the previously reported N,C-chelate compound B(ppy)Mes_2 (ppy = 2-phenylpyridine).[5] However, unlike B(ppy)Mes_2, which undergoes facile and efficient photothermal isomerization between the colorless isomer **a** and the deep-blue isomer **b** only, **1a**−**4a** undergo a sequential multistructural transformation in response to light irradiation or heating. This unusual transformation involves (i) photoisomerization (PI) of **a** to **b**; (ii) thermal intramolecular H-atom transfer (HAT) in **b** to give the new isomer **c**; (iii) a 1,3-shift of the boryl group in **c** to give another new isomer, **d**; and (iv) diastereomer interconversion via ring opening/closing, converting **d** to the new isomer **e** (Scheme 2).

Scheme 1

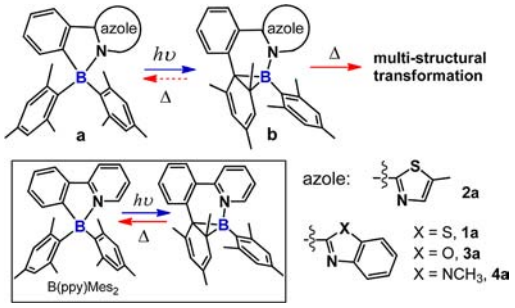

Scheme 2

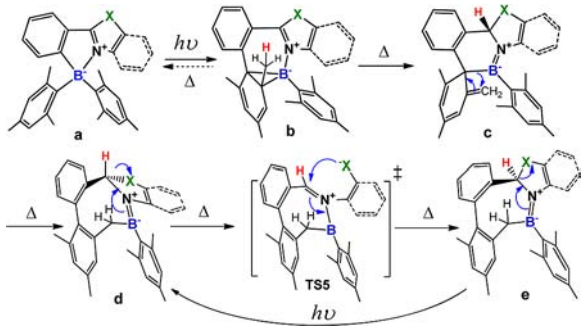

Organoboron compounds that display unusual and unique photo/thermal isomerization phenomena have recently been reported.[5,6] This work further illustrates the exceptional ability of N,C-chelate boron compounds to transform and adapt in response to light and heat.

Compounds **1a**−**4a** were synthesized in good yields by lithiation of the appropriate bromophenylazole or phenylazole

Received: January 31, 2013
Published: February 20, 2013

   dx.doi.org/10.1021/ja400917r | J. Am. Chem. Soc. 2013, 135, 3407−3410

starting materials followed by the addition of $BMes_2F$ and fully characterized by NMR and elemental analyses. Single-crystal X-ray diffraction (scXRD) showed that the structures of **2a** and **3a**[7] are similar to those of $B(ppy)Mes_2$ and its derivatives.[5] Synthetic details, full characterization data for **1a**−**4a**, and crystal data for **2a** and **3a** can be found in the Supporting Information (SI). All four compounds are either colorless or light yellow and are fluorescent with moderate quantum efficiencies (see the SI).

The absorption spectra (Figure 1) and time-dependent density functional theory (TD-DFT) calculations (see the SI)

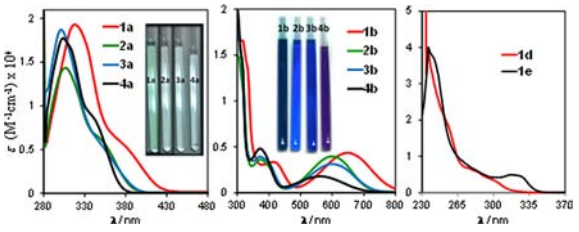

Figure 1. Absorption spectra of (left) **1a**−**4a** in toluene, (middle) their dark isomers **1b**−**4b** in toluene, and (right) **1d** and **1e** in benzene. Inset: Photographs showing the colors of **1a**−**4a** and **1b**−**4b** in C_6D_6.

for **1a**−**4a** indicated that the lowest excited states of these molecules (S_1 and T_1, which are responsible for PI of N,C-chelate $BMes_2$ compounds) have features similar to those of $B(ppy)Mes_2$ and its derivatives.[5c] Thus, not surprisingly, **1a**−**4a**, like $B(ppy)Mes_2$, undergo PI upon irradiation at 350 nm, with a color change to blue, deep blue, or purple (Figure 1), forming **1b**−**4b** quantitatively with moderate PI quantum efficiencies (0.46, 0.35, 0.25, and 0.38, respectively). ^1H and ^{11}B NMR data and DFT calculations confirmed that the structures of **1b**−**4b** are similar to that of the dark isomer of $B(ppy)Mes_2$.

When heated, **1b**−**4b** undergo further isomerization to form **1d**−**4d**, respectively, with **1c**−**4c** as the corresponding intermediates. To illustrate this unusual and complex process, we focus on the transformation of **1b**. The ^1H NMR spectral changes of **1a** upon irradiation and the subsequent changes upon heating are shown in Figure 2. The structures of the isomers and the key transition state involved are shown in Scheme 2. The dark isomer **1b** is transformed into the new species **1c** in solution; the process is slow at ambient temperature and fast upon heating. The most distinct ^1H NMR spectral features of **1c** are the two

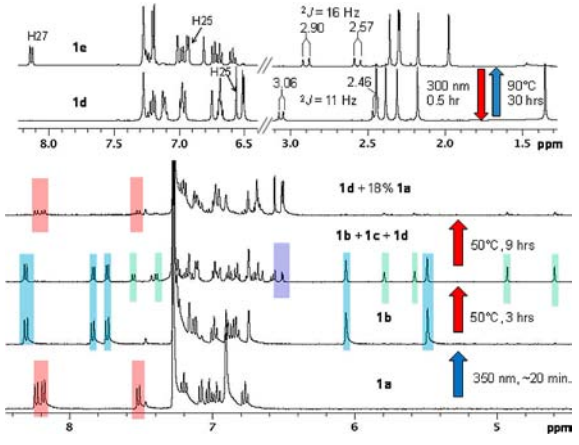

Figure 2. ^1H NMR monitoring of (bottom) the sequential conversions **1a** (red) → **1b** (blue) → **1c** (green) → **1d** (purple) and (top) the interconversion of **1d** and **1e** in C_6D_6.

singlet peaks from the olefinic protons of the cyclohexadienyl (CHD) ring at 5.5−5.8 ppm and the two singlet peaks characteristic of a vinyl group at 4.5−5.0 ppm in C_6D_6. The structure of **1c** was established using 2D NMR spectra and confirmed by DFT calculations and NMR spectra (see the SI). The HAT from a methyl group to C2 of the thiazole ring, transforming the thiazole into a thiazoline, is significant and unusual since the reduction/hydrogenation of azole compounds usually requires a catalyst or the use of a highly reactive hydride.[8] NMR data further showed that **1c** undergoes a subsequent transformation to give **1d** upon prolonged heating; **1d** is stable under ambient air and was isolated and fully characterized by NMR, elemental, and scXRD analyses. The ^1H NMR spectrum of **1d** contains distinct methylene peaks with an AB pattern and $^2J_{H-H}$ = 11 Hz (Figure 2), indicating that **1d** has an asymmetric nature. The ^{11}B NMR chemical shift of **1d** (46.0 ppm) is shifted downfield by >50 ppm relative to that of **1b**, similar to those observed in $Mes_2B{=}NR_2$ and $R_2B{=}NR'_2$ compounds,[9a−e] thus supporting the possible presence of a B=N bond.

The crystal structure of **1d** (Figure 3) confirms the NMR findings unequivocally. C25 of the thiazole ring has been

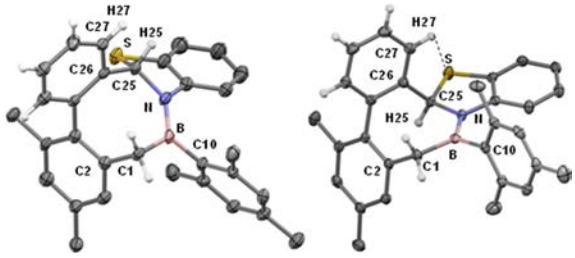

Figure 3. Crystal structures of (left) **1d** and (right) **1e**. Important bond lengths (Å) an angles (deg) for **1d**: B−N, 1.408(7); B−C1, 1.595(9); B−C10, 1.570(7); C1−C2, 1.492(7); C25−C26, 1.509(8); S−C25, 1.822(6); N−C25, 1.508(6); C1−B−C10, 117.8(5); C1−B−N, 121.2(4); C10−B−N, 120.9(5); B−C1−C2, 102.4(5). For **1e**: B−N, 1.424(3); B−C1, 1.597(3); B−C10, 1.579(3); C1−C2, 1.513(3); C25−C26, 1.519(3); S−C25, 1.831(2); N−C25, 1.499(3); C1−B−C10, 113.90(8); C1−B−N, 123.5(2); C10−B−N, 122.50(19); B−C1−C2, 124.17(18).

transformed from an sp^2 carbon to a chiral sp^3 carbon, while the C1 methyl group bound to the aliphatic C atom in **1b** has become a CH_2 group, forming a σ bond with the B atom. The B atom has a trigonal-planar geometry and a B=N bond with a bond length of 1.408(7) Å, which is comparable to some previously reported B=N bond lengths.[9a,d−f] The thiazoline ring is considerably puckered, with a mean deviation of 0.19 Å from the best least-squares plane through the five atoms. H25 is oriented syn with respect to the adjacent phenyl C26−C27 bond. The formation of **1d** arises from a 1,3-sigmatropic shift of the B atom in **1c** driven by rearomatization of the CHD ring (Scheme 2). This leads to an expansion of the six-membered ring in **1c** to an eight-membered ring in **1d**. Although 1,2-sigmatropic migration of organoboron groups is well-known,[10] 1,3-migration as in the **1c** → **1d** transformation is not common.

Most exciting is the quantitative isomerization of **1d** to its diastereoisomer **1e** upon heating at 90 °C, as evidenced by NMR spectra (Figure 2 top). The ^1H NMR spectrum of **1e** is distinctly different from that of **1d**. For example, the H25 peak shifts downfield in going from **1d** to **1e**. The geminal $^2J_{H-H}$ coupling constant of the CH_2 protons becomes much bigger (16 Hz in **1e** vs 11 Hz in **1d**). The crystal structure of **1e** was determined by

dx.doi.org/10.1021/ja400917r | J. Am. Chem. Soc. 2013, 135, 3407−3410

scXRD (Figure 3). One key difference between **1d** and **1e** is the inversion of the configuration of the chiral C atom, C25. As a consequence, H25 becomes anti and the S atom syn to the C26−C27 bond in **1e**. H27 forms an intramolecular hydrogen bond with the S atom (H27···S = 2.89 Å), in agreement with the >1 ppm downfield shift of the H27 peak in the NMR spectrum of **1e** relative to that of **1d** (Figure 2). The C2−C1−B bond angle in **1e** [124.17(18)°] is much greater than that in **1d** [102.4(5)°]. The H−C1−H angle in **1e** (106.3°) is smaller than that in **1d** (111.2°), consistent with the bigger $^2J_{H-H}$ coupling constant of the CH_2 protons. The other key difference between **1d** and **1e** is that the thiazoline ring in **1e** is coplanar with the B, C1, and C10 atoms in **1e** (the mean deviation from the plane defined by the benzothiazoline ring, B, C1, and C10 is 0.052 Å), indicating greater π conjugation of the benzothiazoline and the B atom in **1e** than in **1d**. This is corroborated by the appearance of a distinct low-energy absorption band at 300−350 nm in the UV−vis absorption spectrum of **1e**, which is much weaker and at a slightly higher energy in the spectrum of **1d** (Figure 1). The activation energy for the **1d** → **1e** transformation was determined to be 180 ± 10 kJ mol^{-1} in C_6D_6. Most noteworthy is that fact that the two diastereomers **1d** and **1e** can be interconverted quantitatively (see the SI). **1d** is stable toward irradiation and can be converted to **1e** only thermally. In contrast, **1e** is thermally stable but, remarkably, can be fully converted back to **1d** upon irradiation at 300 nm. This reversible diastereomer interconversion is a rare phenomenon, and it illustrates the possibility of controlling the stereochemistry of azo-heterocyclic molecules with a B unit.

The dark isomers **2b**−**4b** undergo a multistage isomerization process similar to that for **1b**. However, to achieve appreciable thermal transformation of **b** to **d**, higher temperatures are needed for **2b** (90 °C) and **4b** (130 °C). Hence, not surprisingly, the intermediates **2c** and **4c** were not observed in the NMR spectra because of their rapid conversion to **2d** and **4d**, respectively, at the higher temperatures. **3b** can isomerize to **3d** at 50 °C, but the heating time of 30 h needed to achieve the maximum conversion (~100%) is much longer than for **1b**, which reached the maximum conversion to **1d** (~82%) in 9 h at 50 °C. In addition, the **1b** → **1d** isomerization occurs at ambient temperature, while the **3b** → **3d** isomerization was not observed at this temperature. Qualitatively, the **b** → **d** isomerization reactivity follows the order **1b** > **3b** > **2b** ≫ **4b**. The formation of **c** dearomatizes the azole ring in **b**. Thus, the much lower reactivity of **4b** relative to **1b**−**3b** may be due to the aromaticity of the imidazolyl ring in **4b**, which is much greater than that of the azole rings in **1b**−**3b** (see the SI). The fact that the dark isomer of B(ppy)Mes_2 does not undergo intramolecular HAT can also be explained by the well-known high aromaticity of the pyridyl ring. Another important observation is that upon heating, besides isomerizing to **d**, isomers **b** can also thermally revert to the original isomers **1a** (~18%), **2a** (~13%), **3a** (~0%), and **4a** (~82%).

Isomers **2d**−**4d** can be quantitatively converted to **2e**−**4e** at 110, 90, and 130 °C, respectively, in the same manner as **1d** (because of the high temperature used, **4e** was observed in the **4b** → **4d** conversion). However, unlike **1e**, which can be quantitatively converted back to **1d** by irradiation at 300 nm, **2e**−**4e** can be only partially converted back to **2d**−**4d** (max. ~60% for **2d**, ~20% for **3d**, and ~10% for **4d**). Prolonged irradiation of **2e**−**4e** did not increase the conversion yield but instead formed unidentified products that may be caused by either alternative PI pathways of **2e**−**4e** or the poor photostability of **2d**−**4d** (see the SI).

To gain a better understanding of the multistage isomerization process and the difference in the isomerization behaviors of **1a**−**4a**, the mechanistic pathways were investigated using DFT.[11] The results for **1** are shown in Figure 4; those for **2**−**4**, which

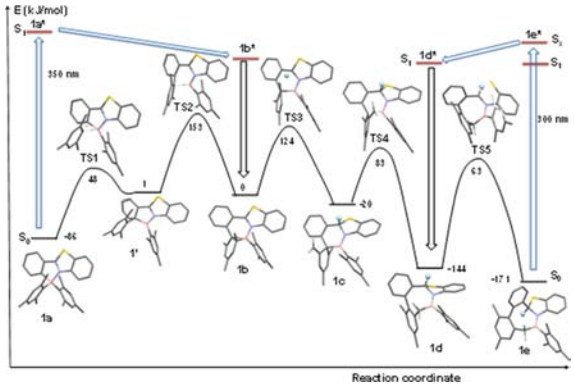

Figure 4. Relative ground-state energies and structures of the isomers, intermediates, and transition states involved in the **1a** → **1e** transformation. The involvement of excited states (S_1 and S_x) in the transformation is also illustrated.

follow the same mechanistic pathway, are given in the SI. The **1a** → **1b** transformation in the ground state follows the same isomerization pathway as established previously for B(ppy)Mes_2 and related compounds.[6c] In the optimized structure of **1b**, the H atom of the methyl group on the BC_2 triangle is ~2.46 Å from the thiazole C2 atom. In the transition state (TS3), the H atom is midway between the methylene and the thiazole C atoms and is transferred directly to the thiazole, forming the syn diastereoisomer **1c** exclusively. The calculated barrier for **1b** → **1a** thermal reversal is ~30 kJ mol^{-1} higher than that for the **1b** → **1c** isomerization, which explains why thermal treatment transforms **1b** predominantly to **1c** instead of **1a**. The activation barrier for the **1c** → **1d** reaction is smaller than that for **1d** → **1c**. Thus, once **1c** is formed, it readily converts to **1d** via TS4, in which the B−C_{CHD} bond is broken and the B atom is roughly equidistant from C_{CHD} and the two vinyl C atoms, supporting a concerted sigmatropic migration of the B group.

The most important finding from the computational work is that the **1d** → **1e** conversion involves the transition state TS5 (Scheme 2 and Figure 4), in which the C−S bond dissociates, a C═N bond forms, and the B═N bond becomes a B−N bond. The structure of TS5 is reminiscent of the ring-opened isomer of spiropyrans and related compounds.[4a,12] The C−S bond dissociation is the key for the configuration inversion of the chiral carbon atom and the interconversion of **1d** and **1e**. The ability of the B center to accommodate both B−N and B═N bonds likely also plays an important role in this reversible isomerization. The barrier for the **1d** → **1e** reaction is much higher than that for the **1b** → **1c** (**1d**) process, in agreement with the higher temperature needed for the **1d** → **1e** conversion. Isomer **1e** is ~27 kJ mol^{-1} more stable than **1d**, which may explain the inability of **1e** to undergo thermal reversion to **1d**. The S_1 state of **1e** is below that of **1d**, and the HOMO → LUMO transition dominates the S_1 state for both compounds. However, the oscillator strength for **1e** is ~5 times greater than that for **1d**, in agreement with the UV−vis spectrum (Figure 1). Thus, **1e** must be excited above the S_1 state for it to be converted effectively to **1d** in the excited state. It is conceivable that a transition state similar to TS5 is involved in the excited-state

dx.doi.org/10.1021/ja400917r | J. Am. Chem. Soc. 2013, 135, 3407−3410

conversion of **1e** to **1d**, requiring the B═N bond to change into a B−N bond and the C−S bond to break. Thus, to achieve effective PI of **1e** to **1d**, the HOMO should be localized on the B═N bond and the thiazoline unit, which is indeed the case for **1e**. In contrast, for **1d**, there is a large contribution to the HOMO from the dimethylbenzene ring (the C2 ring in Figure 3), which may explain the inability of **1d** to photoisomerize to **1e**. The calculations also showed that among **1a**−**1e**, the thiazoline isomers **1d** and **1e** have the lowest energy. Thus, the unusual multistructural transformation is thermodynamically favored.

The calculated barriers for the **b** → **c** conversions follow the order **1b** < **3b** ≈ **2b** < **4b**, in agreement with the experimentally observed reactivity trend. The relative stability of **c** versus **b** (i.e., the energy difference of the two isomers) follows the order **1c** (−20 kJ mol^{-1}) > **3c** (−6 kJ mol^{-1}) > **2c** (5 kJ mol^{-1}) > **4c** (25 kJ mol^{-1}). The poor stability of **4c** and the high **4b** → **4c** activation barrier are consistent with the relatively high aromaticity of the imidazolyl ring and are responsible for the low activity of the **4b** → **4d** isomerization. The greater activity of the **1b** → **1d** conversion compared with the **3b** → **3d** conversion, despite the somewhat lower aromaticity of the benzoxazole ring in **3b**, may arise because weaker oxazole N donor in **3b** stabilizes TS3 less effectively than the thiazole N donor in **1b**. The observed reactivity trend for **b** → **d** conversion likely results from both aromaticity and the azole N donor strength. The activation barriers of the **b** → **a** thermal reversal follow the order **1b** < **2b** < **3b** ≈ **4b**, and the relative stability of **a** versus **b** follows the order **4a** > **1a** ≈ **2a** > **3a**, which, along with the **b** → **c** reactivity trend, is responsible for the observed relative distribution of **a** and **d**/**e** in the thermal isomerization of **b**.

In summary, an unprecedented multistructural transformation of B(2-phenylazolyl)Mes_2 compounds has been demonstrated, and mechanistic pathways for this remarkable phenomenon have been established. Because the formation of the dark isomer **b** is the key for the subsequent transformation, this work demonstrates that light can be used as a convenient trigger or switch to turn on unusual and complex structural/chemical transformations of organoboron compounds. The intramolecular HAT observed in this system is facilitated by the relatively low aromaticity of the azole rings. The ability of a BRR′ unit to accommodate both B═N and B−N bonds plays a key role in promoting the reversible isomerization of **d** and **e**, illustrating the potential use of organoboron chromophores in controlling stereoselective ring-opening/closing processes of azole heterocycles.

■ ASSOCIATED CONTENT

Supporting Information

Synthesis and computational details, additional results, and complete ref 11 (as ref 6S). This material is available free of charge via the Internet at http://pubs.acs.org.

■ AUTHOR INFORMATION

Corresponding Author

wangs@chem.queensu.ca

Notes

The authors declare no competing financial interest.

■ ACKNOWLEDGMENTS

We thank the Natural Sciences and Engineering Research Council of Canada for financial support and the High Performance Computing Virtual Laboratory for computing facilities. S.W. thanks the Canada Council for the Arts for the Killam Research Fellowship. Y.-L.R. thanks the Government of Canada for the Vanier Scholarship.

■ REFERENCES

(1) (a) Woolley, G. A. *Nat. Chem.* **2012**, *4*, 75. (b) Beharry, A. A.; Woolley, G. A. *Chem. Soc. Rev.* **2011**, *40*, 4422. (c) Balzani, V.; Credi, A.; Venturi, M. *Molecular Devices and Machines*; Wiley-VCH: Weinheim, Germany, 2003. (d) Feringa, B. L. *Molecular Switches*; Wiley-VCH: Weinheim, Germany, 2001.

(2) (a) Natansohn, A.; Rochon, P. *Adv. Mater.* **1999**, *11*, 1387. (b) Natansohn, A.; Rochon, P. *Chem. Rev.* **2002**, *102*, 4139. (c) Kume, S.; Nishihara, H. *Dalton Trans.* **2008**, 3260. (d) Yokoyama, Y.; Saito, M. In *Chiral Photochemistry*; Inoue, Y., Ramamurthy, Y., Eds.; Marcel Dekker: New York, 2004; Chapter 6.

(3) (a) Cölle, M.; Dinnebier, R. E.; Brütting, W. *Chem. Commun.* **2002**, *23*, 2908. (b) Cölle, M.; Gmeiner, J.; Milius, W.; Hillebrecht, H.; Brütting, W. *Adv. Funct. Mater.* **2003**, *13*, 108. (c) Tamayo, A. B.; Alleyne, B. D.; Djurovich, P. I.; Lamansky, S.; Tsyba, I.; Ho, N. N.; Bau, R.; Thompson, M. E. *J. Am. Chem. Soc.* **2003**, *125*, 7377.

(4) (a) Berkovic, G.; Krongauz, V.; Weiss, V. *Chem. Rev.* **2000**, *100*, 1741 and references therein. (b) Irie, M. *Chem. Rev.* **2000**, *100*, 1685. (c) Ko, C.-C.; Yam, V. W.-W. *J. Mater. Chem.* **2010**, *20*, 2063.

(5) (a) Rao, Y. L.; Amarne, H.; Zhao, S. B.; McCormick, T. M.; Martic, S.; Sun, Y.; Wang, R. Y.; Wang, S. *J. Am. Chem. Soc.* **2008**, *130*, 12898. (b) Amarne, H.; Baik, C.; Murphy, S. K.; Wang, S. *Chem.—Eur. J.* **2010**, *16*, 4750. (c) Rao, Y. L.; Amarne, H.; Wang, S. *Coord. Chem. Rev.* **2012**, *256*, 759. (d) Rao, Y. L.; Amarne, H.; Lu, J. S.; Wang, S. *Dalton Trans.* **2013**, *42*, 638.

(6) (a) Ansorg, K.; Braunschweig, H.; Chiu, C. W.; Engels, B.; Gamon, D.; Hügel, M.; Kupfer, T.; Radacki, K. *Angew. Chem., Int. Ed.* **2011**, *50*, 2833. (b) Wilkey, J. D.; Schuster, G. B. *J. Am. Chem. Soc.* **1988**, *110*, 7569. (c) Rao, Y.-L.; Chen, L. D.; Mosey, N. J.; Wang, S. *J. Am. Chem. Soc.* **2012**, *134*, 11026. (d) Nagura, K.; Saito, S.; Fröhlich, R.; Glorius, F.; Yamaguchi, S. *Angew. Chem., Int. Ed.* **2012**, *51*, 7762. (e) Fukazawa, A.; Yamaguchi, E.; Ito, E.; Yamada, H.; Wang, J.; Irle, S.; Yamaguchi, S. *Organometallics* **2011**, *30*, 3870. (f) Fukazawa, A.; Yamada, H.; Yamaguchi, S. *Angew. Chem., Int. Ed.* **2008**, *47*, 5582. (g) Kano, N.; Yoshino, J.; Kawashima, T. *Org. Lett.* **2005**, *7*, 3909. (h) Yoshino, J.; Kano, N.; Kawashima, T. *Tetrahedron* **2008**, *64*, 7774. (i) Wakamiya, A.; Taniguchi, R.; Yamaguchi, S. *Angew. Chem., Int. Ed.* **2006**, *45*, 3170.

(7) The crystal structure data files for **2a**, **3a**, **1d**, and **1e** have been deposited at the Cambridge Crystallographic Data Centre (CCDC 913143, 913142, 913141, and 913144, respectively).

(8) (a) *Thiazole and Its Derivatives*; Metzger, J. V., Ed.; The Chemistry of Heterocyclic Compounds, Vol. *34*; Wiley: New York, 1979; Part I, pp 132−133. (b) Hofmann, K. *Imidazole and Its Derivatives, Part I*; The Chemistry of Heterocyclic Compounds, Vol. *6*; Interscience: New York, 1953. (c) Clarke, G. M.; Sykes, P. *J. Chem. Soc. C* **1967**, 1411. (d) Katritzky, A. R.; Ramsden, C. A.; Joule, J. A.; Zhdankin, V. V. *Handbook of Heterocyclic Chemistry*, 3rd ed.; Elsevier: Oxford, U.K., 2010; Chapter 3.4, p 535.

(9) (a) Cui, Y.; Li, F. H.; Lu, Z. H.; Wang, S. *Dalton Trans.* **2007**, 2634. (b) Robertson, A. P. M.; Leitao, E. M.; Manners, I. *J. Am. Chem. Soc.* **2011**, *133*, 19322. (c) Brown, N. M. D.; Davidson, F.; Wilson, J. W. *J. Organomet. Chem.* **1980**, *192*, 133. (d) Pestana, D. C.; Power, P. P. *Inorg. Chem.* **1991**, *30*, 528. (e) Lichtblau, A.; Hausen, H. D.; Schwarz, W.; Kaim, W. *Inorg. Chem.* **1993**, *32*, 73. (f) Okada, K.; Suzuki, R.; Oda, M. *J. Chem. Soc., Chem. Commun.* **1995**, 2069.

(10) (a) Bromm, L. O.; Laaziri, H.; Lhermitte, F.; Harms, K.; Knochel, P. *J. Am. Chem. Soc.* **2000**, *122*, 10218. (b) Varela, J. A.; Pena, D.; Goldfuss, B.; Polborn, K.; Knochel, P. *Org. Lett.* **2001**, *3*, 2395. (c) Wood, S. E.; Rickborn, B. *J. Org. Chem.* **1983**, *48*, 555.

(11) Frisch, M. J.; et al. *Gaussian 09*, revision B.01; Gaussian, Inc.: Wallingford, CT, 2010.

(12) (a) Toman, P.; Bartkowiak, W.; Nešpůrek, S.; Sworakowski, J.; Zaleśny, R. *Chem. Phys.* **2005**, *316*, 267. (b) Paramonov, S. V.; Lokshin, V.; Fedorova, O. A. *J. Photochem. Photobiol., C* **2011**, *12*, 209.